Significance of poly(ethylene terephthalate) (PET) substrate crystallinity on enzymatic degradation

Thomsen, Thore Bach; Almdal, Kristoffer; Meyer, Anne S.

Published in:
New Biotechnology

Link to article, DOI:
10.1016/j.nbt.2023.11.001

Publication date:
2023

Document Version
Publisher's PDF, also known as Version of record

New BIOTECHNOLOGY 78 (2023) 162–172

Contents lists available at ScienceDirect

New BIOTECHNOLOGY

journal homepage: www.elsevier.com/locate/nbt

Review article

Significance of poly(ethylene terephthalate) (PET) substrate crystallinity on enzymatic degradation

Thore Bach Thomsen [a], Kristoffer Almdal [b], Anne S. Meyer [a,*]

[a] Department of Biotechnology and Biomedicine, DTU Bioengineering, Protein Chemistry and Enzyme Technology Section, Building 221, Technical University of Denmark, 2800 Kgs Lyngby, Denmark
[b] DTU Chemistry, Building 206, Technical University of Denmark, 2800 Kgs Lyngby, Denmark

ARTICLE INFO

Keywords:
Polyester
Plastic bottles
Substrate crystallinity
PET hydrolases
PET recycling

ABSTRACT

Poly(ethylene terephthalate) (PET) is a semi-crystalline plastic polyester material with a global production volume of 83 Mt/year. PET is mainly used in textiles, but also widely used for packaging materials, notably plastic bottles, and is a major contributor to environmental plastic waste accumulation. Now that enzymes have been demonstrated to catalyze PET degradation, new options for sustainable bio-recycling of PET materials via enzymatic catalysis have emerged. The enzymatic degradation rate is strongly influenced by the properties of PET, notably the degree of crystallinity, X_C. The higher the X_C of the PET material, the slower the enzymatic rate. Crystallization of PET, resulting in increased X_C, is induced thermally (via heating) and/or mechanically (via stretching), and the X_C of most PET plastic bottles and microplastics exceeds what currently known enzymes can readily degrade. The enzymatic action occurs at the surface of the insoluble PET material and improves when the polyester chain mobility increases. The chain mobility increases drastically when the temperature exceeds the glass transition temperature, T_g, which is ~40 °C at the surface layer of PET. Since PET crystallization starts at 70 °C, the ideal temperature for enzymatic degradation is just below 70 °C to balance high chain mobility and enzymatic reaction activation without inducing crystal formation. This paper reviews the current understanding on the properties of PET as an enzyme substrate and summarizes the most recent knowledge of how the crystalline and amorphous regions of PET form, and how the X_C and the T_g impact the efficiency of enzymatic PET degradation.

Introduction

Plastic pollution has become a global environmental concern due to the ubiquitous presence of plastics within aquatic and terrestrial environments [1,2]. Nevertheless, the annual demand for plastics keeps increasing by 3–4% per year, and the global annual production of plastics reached ~390 Mt in 2021 (excluding plastics used in textile fibers), with 90% produced from fossil-based feedstock [3]. By including the production of synthetic textile fibers, which amounts to 68.2 Mt/year [4], total global plastic production is nearly ~460 Mt/year.

Poly(ethylene terephthalate) (PET) is a semi-crystalline type of polyester plastic, which is mainly used for textile fibers, but also renowned as the most widely used type of plastic used for plastic bottles, notably single-use bottles for soft drinks and water [3,5]. Such single-use plastic bottles are categorized as post-consumer packaging materials. Because of their short lifespan and low collection rate, post-consumer packaging materials are major contributors to plastic pollution. The total annual production of post-consumer packaging materials is currently 72 Mt, of which 32% is leaked outside the collection system [6], and ultimately ending up as plastic pollution in both marine and terrestrial environments [7].

Various regional, national, and global policies have been implemented to mitigate plastic pollution and promote a circular economy of plastics [8,9]. To highlight the urgency, it is noted that the European Union Directive (EU) 2019/904 has set a collection target of 90% of single-use plastics by 2029, as well as a requirement that, by 2025, at least 25% of plastic bottles within the EU contain recycled plastics (30% by 2030) [10].

Abbreviations: BHET, Bis(2-Hydroxyethyl) terephthalate; EG, ethylene glycol; MAF, mobile amorphous fraction; MHET, mono(2-hydroxyethyl)terephthalic acid; RAF, rigid amorphous fraction; *Tg*, glass transition temperature; TPA, terephthalic acid; X_C, degree of crystallinity.

* Corresponding author.
E-mail address: asme@dtu.dk (A.S. Meyer).

https://doi.org/10.1016/j.nbt.2023.11.001
Received 26 August 2023; Received in revised form 20 October 2023; Accepted 4 November 2023
Available online 7 November 2023

PET is manufactured at a global production volume of ~83 Mt/year, thus constituting 52% of the total global fiber production [4] and 6.2% of the global plastic production (textiles excluded) [3]. Despite PET being the most recycled plastic type [11], with plastic bottle recycle rates of up to 96% (e.g., in Denmark), the newest PET production data from Europe include only about 25% recycled PET [12]. Although this recycling rate indicates a profound increase in recycling [12], it is indisputable that most of the globally produced PET is synthesized from scratch from fossil oil via oxidation of the aromatic hydrocarbon *p*-xylene, derived directly from petroleum, to terephthalic acid (TPA) [13]. The PET polyester resin is then obtained by esterification or transesterification between TPA or dimethyl terephthalate and ethylene glycol (EG), followed by polymerization [14]. For use as packaging material or bottles, the PET resin is manufactured to the desired shape via injection molding (blow-molding) or extrusion. A recent life-cycle-assessment of PET bottles showed that 84% of the environmental burden quantified in terms of resource consumption, climate change, ecosystem quality, and human health is caused by the production of PET resin [5].

To address the negative environmental impact of plastics - including PET - there is an urgent need to drastically intensify sustainable recycling efforts. The conventional methods for recycling of PET principally involve mechanical and thermal treatment, i.e., washing and shredding of the material, and then regranulation via extrusion [15]. In the case of PET, this type of mechanical recycling typically results in a lower quality of the recycled product compared to the original (virgin) material. Specifically, the treatment causes changes in appearance, meaning color and brittleness, and in material properties at the molecular level such as lower molecular weight (M_w), polymer chain length (M_n), and polydispersity index (M_w/M_n), resulting in decreased tensile strength. The crystallization rates of recycled PET also increase leading to a higher X_C of the re-processed products [16–18]. In fact, 27% of the recycled PET from Europe has only limited uses due to its poor quality [12]. In addition, the existing commercially viable recycling processes are constrained to certain PET products, as not all PET products can be effectively recycled by classic means. This includes textile blends of different fiber types such as polyester, cotton, etc., which are common in clothing and other textile fabrics [19].

Development and implementation of new technologies are therefore clearly required in order to facilitate higher recycling rates and improve the quality of the recycled products [20]. Plastics, including PET, are considered resistant to biodegradation. However, the realization that certain enzymes and microbes can catalyze degradation of PET [21–23], has significantly boosted the efforts for sustainable PET recycling, notably recycling of PET plastic bottles, yielding high quality recycled products [24]. PET degrading enzymes may also be used to recycle textile blends by specifically degrading the PET polyester fibers alone or in combination with other enzymes that target other fibers in the material, such as cellulases that target cotton, or in combination with a chemical pretreatment [19,25].

While the continued discovery and protein engineering of efficient PET degrading enzymes have created novel opportunities for industrial biotechnology-based PET recycling, it has become evident that the activity of the PET degrading enzymes is strongly influenced by the physical properties of PET, notably the degree of crystallinity (X_C). The X_C is defined as the fraction of the total PET polymer chains that are in the crystalline structure state [26–28]. In addition, the surface glass transition temperature, T_g, of PET and the local mobility of the amorphous PET chains affect the amenability of PET to enzymatic attack and degradation. This paper reviews the enzymatic conversion of PET with particular emphasis on the distinct complexity of PET as a semi-crystalline substrate for enzymatic depolymerization.

Enzymatic recycling of PET

The use of plastic degrading enzymes in biocatalysis-based recycling of PET has recently been introduced as a new promising technology enabling the production of recycled products of the same quality as the virgin PET plastic materials [29], and enzyme-based technology has already shown great potential for industrial-scale PET recycling, thus allowing for closed-loop circular economy processes [27,30]. In addition, unlike thermo-mechanically recycled PET, the enzyme-based approach permits the degradation products to be used as feedstock for the manufacture of other products, including other types of polyester materials such as polyhydroxy alkanoates (PHAs) [31].

Although plastics are man-made polymers, several enzymes are capable of degrading synthetic polyesters, even if they are not their natural substrate [32–34]. The PET hydrolase class, EC 3.1.1.101, was created in 2016 based on the discovery of the PET degrading enzyme enabling *Ideonella sakaiensis* 201-F6 to utilize PET as its major carbon source [23]. For the sake of completeness, it is noted that *I. sakaiensis* 201-F6 also secretes a MHETase (EC 3.1.1.102), which catalyzes the further conversion of mono(2-hydroxyethyl)terephthalic acid (MHET), a product of the PET hydrolase reaction, into TPA and EG [23,35]. Despite the existence of the PET hydrolase class, the vast majority of PET degrading enzymes are classified as cutinases (EC 3.1.1.47) [36–38] or carboxyl esterases (EC 3.1.1.1) [39]. In addition, certain arylesterases [40] (EC 3.1.1.2) and lipases [26] (EC 3.1.1.3) are also known to be active on PET.

An overview of characterized PET hydrolases is listed in different online databases, i.e., the PaZy [39], the PlasticDB [41], and partly the PMBD database (the PMBD database has a lot fewer entries than the other two and the PaZy database has the most) [42]. By studying the database entries it is evident that the majority of the currently characterized PET degrading enzymes originate from either the *Actinobacteriota* or the *Pseudomonadota* phyla. A phylogenetic tree covering all entries from the PaZy database with their microbial origin (phylum level) and EC numbers, is displayed in Fig. 1. Despite having a PET hydrolase EC number, EC 3.1.1.101, the IsPETase clearly shares a cluster with other carboxyl esterases. This phylogenetic tree also displays the dominance of hitherto known PET degrading enzymes originating from Actinobacteria (grey nodes) and Pseudomonadota (turquoise blue nodes), but also reveals that enzymes that have some activity on PET are found in a range of different microbial organisms, including archae (Genbank Accession no. **RLI42440**, a feruloyl esterase type of enzyme) and fungi (Genbank Accession no. **AAA33335.1** and **A0A075B5G4**, which are cutinases originating from a *Fusarium* spp. and a *Humicola* spp., respectively) [39]. This variety signifies the diversity of PET hydrolyzing enzymes and underscores the likely possibility that several more may be discovered in the future.

Features of PET as a semi-crystalline, thermoplastic material

PET consists of repeating units of TPA and EG, covalently bound via ester bonds, and it is the hydrolysis of the ester bonds that is catalyzed by PET degrading enzymes. In the melt state above the melting temperature, T_m, (260 °C) PET is a disordered random coil polymer melt. If the melt is cooled sufficiently quickly - quenched - to temperatures below the T_g of PET, then the amorphous random coil structure is preserved; as discussed later, the T_g of PET is ~65–75 °C for amorphous bulk PET [28,43,44], with some variation depending on the methodological procedure used. However, solid PET is usually in a semi-crystalline state which contains both highly ordered domains (crystals) as well as glassy amorphous domains. It is the amount of crystals, i.e. the level of highly ordered crystalline domains, which defines the X_C of PET polyester materials [45]. Although high cooling rates are readily achievable in standard processing operations, the material properties such as gas permeability of amorphous PET are not always desirable for the material use [46]. Hence, PET products, including plastic bottles and textile fibers, tend to have a high X_C [47,48].

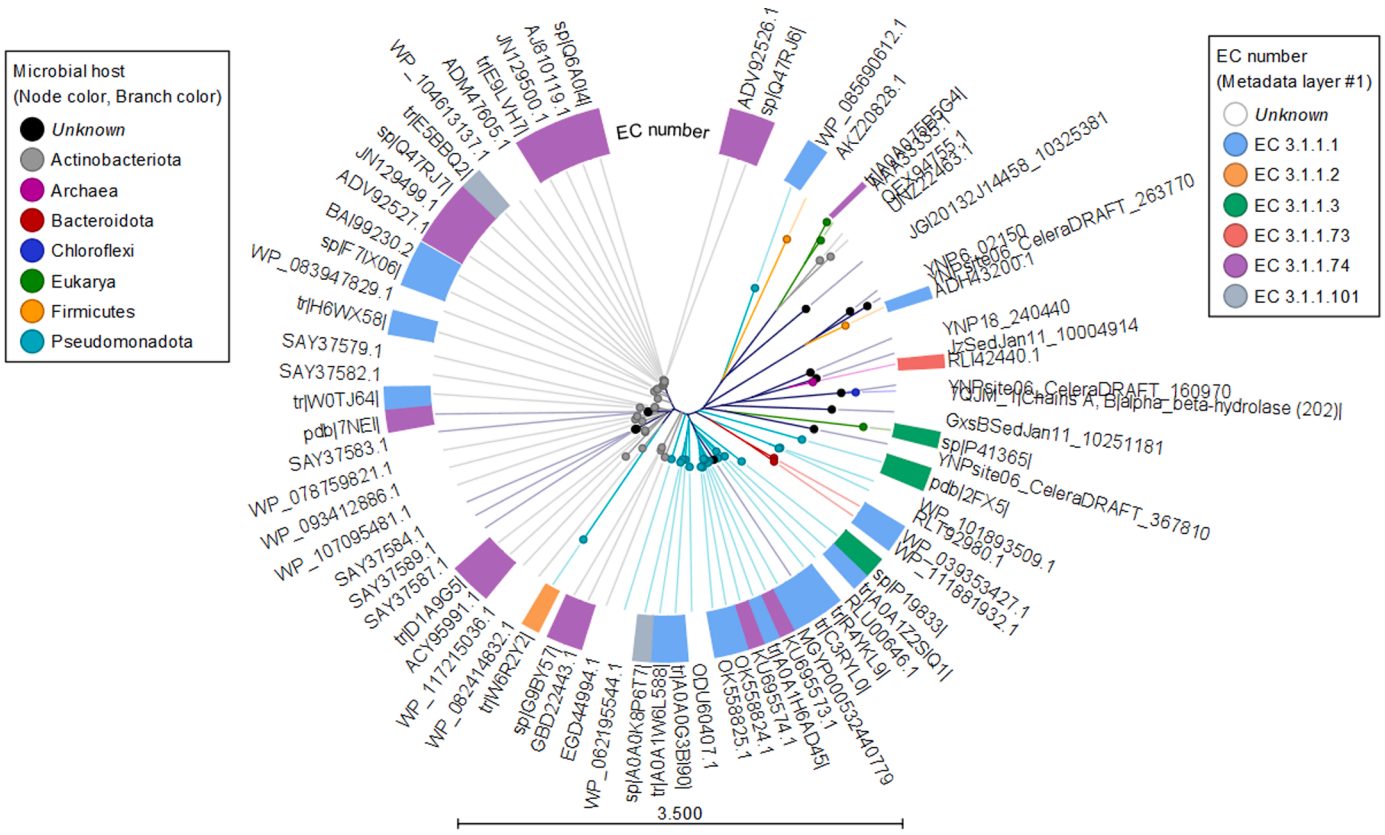

Fig. 1. Phylogenic tree of all currently characterized PET hydrolases. The phyla of the microbial host are indicated by node color, while the EC number is highlighted by the surrounding colors of the tree (The tree was prepared using CLC Main Workbench 8 from Qiagen (Hilden, Germany) .

Crystallization of PET

The crystalline regions - or crystals - in PET material form when the polymeric chains in the amorphous state align, which in turn happens when the chain mobility/energy of the material is sufficiently high. A high chain mobility/energy can be achieved by either thermal or mechanical means, which is why heating and mechanical molding lead to the formation of crystals, and thus an increase in the X_C of the PET material [49]. Thermally induced crystallization takes place at temperatures above the T_g [50] (for PET sheets thicker than 100 nm typically at temperatures above 70 °C for surface crystals to form, and 85 °C for bulk crystals to form [51]), and notably occurs when the PET material is slowly cooled from melt or kept at temperatures above the T_g. The crystallization process is quenched by cooling the material to a temperature below the T_g of PET. The rate at which the crystallization occurs increases with temperature, until it reaches its maximum at 174 °C [43]. Beyond this temperature, the crystallization rate starts to decrease due to excessive chain mobility. On the other hand, at temperatures below T_g, the mobility of the chains is restricted, leading to limited crystallization [50]. Other factors such as moisture content [52] and molecular weight of the polymers in the PET material [53] also influence the crystallization of PET.

The mechanically induced crystallization of PET is typically induced via stretching the material. This process is referred to as stress or strain induced crystallization, and requires stretching of the PET material at temperatures above T_g [49]. The X_C caused by strain induced crystallization increases with both temperature and strain rate [54]. The increased crystallinity can lead to improvements in the mechanical properties of PET material such as higher modulus, toughness, stiffness, tensile strength, and hardness [55]. The ability of changing the X_C, and hence the mechanical properties of PET by strain induced crystallization is utilized in many applications of PET processing, most notably in the manufacturing of blow-molded PET bottles, textile fibers, and oriented films [56]. The X_C of a PET material is therefore heavily dependent on its processing history and due to the changes taking place at the molecular chain level, the X_C may not be uniform throughout a PET material. An example of this is illustrated by the X_C of a PET bottle [48], presented in Fig. 2. Here it is evident that the finish/neck and base center have a lower X_C (1.2% and 11.7%, respectively) than the rest of the bottle, that has $X_C > 25\%$ [48]. Furthermore, plastic waste in the environment, including microplastics, may undergo weathering/aging because of solar exposure and thermal aging, which increases the X_C [57].

Details of the structure and morphology of PET crystals

During crystallization, the PET chains undergo a conformational change from a predominantly *trans-gauche-trans* to a linear all-*trans* conformation; a schematic representation of the all-*trans* conformation of a PET chain is shown in Fig. 3A. Although the linear all-*trans* conformation of the free PET chain is energetically less favorable than a

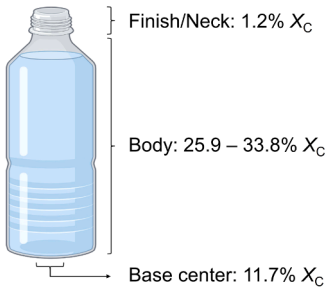

Fig. 2. The degree of crystallinity (X_C) varies in different regions of a PET bottle. The figure is a schematic adaptation of data presented by Lu et. al. [48].

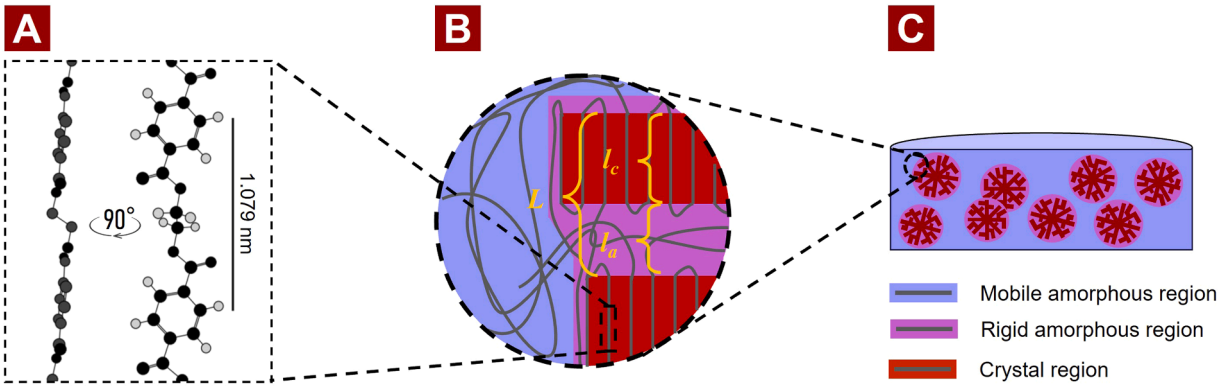

Fig. 3. Schematic representation of the structural details of the crystal structure of a PET crystal within semi-crystalline PET: A) side and front view of the all-*trans* molecular confirmation of a structural moiety (two TPA and one EG moiety) of the polymeric chain of a PET crystal; B) Molecular arrangement and lamellar structure of the polymeric chains in semi-crystal PET (l_a, l_c, and L, are explained in the text); C) Schematic representation of the spherical crystalline regions in a semi-crystalline PET material.

trans-gauche-trans conformation, the all-*trans* confirmation of a crystal structure is stabilized by intermolecular π/π stacking of the aromatic rings of the TPA moieties, which is why the all-*trans* is the prevalent chain conformation in PET crystals [58]. In other words, this means that there is a decrease in *gauche* conformations with increasing X_C [59,60]. The unit cell structure of PET crystals has been extensively studied, and has been shown to form triclinic crystals [61]. However, the unit cell parameters of PET crystals are not universal, as they are highly dependent on the crystallization and manufacturing process parameters. These parameters include the crystallization temperature, draw ratio, and subsequent annealing temperature and time [61].

Within a PET crystal the polymer chains are arranged in densely packed lamellae structures. These crystalline lamellae are separated by amorphous regions, and interconnected by PET chains, known as tie molecules, which are crossing the crystal-amorphous interface [62]. As illustrated in Fig. 3B, the morphological parameters of a PET crystal may be quantified in terms of the average crystalline lamellae thickness (l_c), the average interlamellar amorphous layer thickness (l_a), and the long period (L), which is the sum of l_c and l_a [63] (Fig. 3B). Due to the effect of temperature and mechanical stress on the crystallization, the morphology of the PET crystal, and hence the values of l_c, l_a, and L are obviously highly dependent on the crystallization process and the processing conditions [63,64].

The crystallization of PET can be divided into nucleation and crystal growth. During nucleation, amorphous PET chains align in the lamellar structure, thus forming the nucleus of a new crystal. The formation of nuclei is followed by the development of the crystals, the crystal/lamellae growth phase. The growth phase can be further divided into two stages, primary and secondary crystallization. Primary crystallization designates the initial stage of crystal growth, which is associated with growth of the heterogeneous crystal structures (as outlined below, this entails that the lamellae and the rigid amorphous fraction structures expand the boundaries of the PET crystal). The secondary crystallization takes place within the boundaries of a crystal structure, and is associated with either thickening (increase in l_c and reduction in l_a) of the lamellae structures and/or formation of new lamellae within a crystal (formation of spherulites) [43,65]. The crystalline lamellae are furthermore arranged in a higher-level structure. The anatomy of the higher-level structure is also dependent on the crystallization process [51,66,67]. A simplified representation of the lamellar crystal structures and distribution of the crystal structures is illustrated in Fig. 3C.

Thermally induced crystals manifest as highly branched spherulites (bulk crystals) or as micelles (surface crystals) [45,66,68]. The size of these crystals is influenced by the annealing temperature, as larger crystals are formed at higher temperatures [50,66]. The visual appearance of thermally annealed PET samples becomes progressively more opaque with increasing X_C, resulting from the increased light scattering caused by the crystals [69]. Studies by *in situ* Atomic Force Microscopy of the annealing of spin coated PET film (thickness up to 680 nm), have revealed that surface crystals begin to form at 70 °C, whereas crystal formation in the bulk material starts at 85 °C [51]. However, no bulk crystals were observed on films thinner than 10 nm within a temperature range of 50–190 °C [51]. In contrast to thermally induced crystals, the crystal structures resulting from strain induced crystallization are generally elongated in rod-like or fibrillary structures [67]. Here, the lamella are oriented in the direction of the strain, while the lamellar structures following thermally induced crystals are oriented randomly [64]. The crystal size of PET samples which have undergone strain induced crystallization are moreover smaller than thermally induced crystals. PET material with stress/strain induced crystals may therefore appear transparent due to the small crystal size [49].

Amorphous fractions

In its melt form the PET chains adopt a disordered random coil-state, as mentioned above. These chains are highly flexible, leading to highly entangled structures. The entanglement molecular weight (MW_e) of PET, which is a measure of the molecular weight between two chain entanglements, is typically between 1450 and 2120 g/mol [70] corresponding to an entanglement between every 7.5–11 repeating units (i.e., the mono(2-hydroxyethyl) terephthalate MHET units) in a PET chain. This amorphous state of the polymeric chains is maintained in the solid state if the polymer melt is cooled rapidly to temperatures below the T_g.

The amorphous fraction of PET can be further divided into two different fractions, namely a mobile amorphous fraction (MAF) and a rigid amorphous fraction (RAF). The MAF consists of the amorphous regions between the crystal structures, while the RAF is associated with the interface between the crystal and the amorphous regions (Fig. 3B). This interface also includes the interlamellar spacing within PET crystals (quantified as l_a, Fig. 3B). Therefore, the RAF content of a PET sample increases with the X_C, while the MAF content decreases [49,71,72]. The RAF and MAF content of a PET sample is also affected by the crystal morphology [73]. A recent study has shown that the RAF content in a biaxially oriented PET film was higher than in thermally annealed samples (at 120 and 190 °C), even though the X_C was highest in biaxially oriented PET film [64]. Compared to the chains in the MAF, the mobility of the chains within the RAF is physically restrained by the crystal lamellae as shown in Fig. 3B. As a consequence, the RAF remains in its glass-state, while the MAF transitions into the mobile rubber-state once heated above the T_g value [71]. The overall T_g of PET may be lowered by the presence of additives [74] or by absorption of water molecules, conferring a plasticizing effect on PET [75,76], that impact the

enzymatic attack and hence the enzymatic depolymerization of PET, to be discussed further below.

The enzymatic degradation mechanism on semi-crystalline PET

By studying PET chain length distribution using MALDI-TOF and the changes in surface chemistry by X-ray photoelectron spectroscopy (XPS) of enzyme treated PET with a lipase and a cutinase, respectively, Eberl et. al. proposed that the enzymatic degradation of the insoluble PET was facilitated predominantly by random (endo-type) chain scissoring [77]. This interpretation was based on the observations that the enzymatic treatment of PET increased the surface polarity, and increased the level of smaller insoluble fragments (fewer than 11 TPA moieties) in the insoluble substrate [77]. They furthermore demonstrated that the degradation pattern differed between two PET degrading enzymes, as one (the *Thermobifida fusca* cutinase) appeared have a higher preference for chain scissoring at the terminal, exo-type, releasing more soluble products than the other enzyme (the *Thermomyces lanuginosus* lipase), which instead accumulated more smaller insoluble fragments, indicating a higher preference for endo-type chain scissoring [77].

During enzymatic degradation of PET, the insoluble polymeric chains are ultimately hydrolyzed into smaller soluble products. These degradation products are primarily EG, TPA, MHET, and to a lesser extent Bis(2-Hydroxyethyl) terephthalate (BHET) [29,78], but larger PET oligomers containing two or more aromatic rings have also been observed [26,79,80]. Concurrently with the heterologous catalysis of the insoluble PET chains, the soluble degradation products can undergo further degradation through homogenous catalysis. This simultaneous heterogeneous and homogeneous enzymatic catalysis occurs as the PET degrading enzymes are also capable of degrading the soluble products, although different PET degrading enzymes have been found to attack the soluble substrates such as BHET and MHET at different rates [79,81,82].

The progression of the product profile of PET during degradation by PET degrading enzymes was recently studied in more detail by Schubert et. al [79] who, using stochastic modeling, predicted the reaction pathways of four different PET hydrolyzing enzymes, in terms of their course of reaction and evolution in product formation. The work showed that efficient PET hydrolases (notably exemplified by the LCC enzyme) were characterized by showing a higher extent of endo-type chain scissoring that did not result in the immediate release of soluble products [79]. A degradation mechanism taking the crystalline and amorphous regions of PET into consideration was recently updated by Wei and coworkers [83]. They suggested that the MAF regions could be degraded by both endo- and exo-type chain scission, while the RAF and PET crystals can only be degraded via endo-type scission. This hypothesis was deducted by an assessment of the molecular weight distribution of enzymatically treated PET samples [83]. A schematic representation of this mechanism is presented in Fig. 4.

It has also recently been shown that no soluble products are released during the initial enzyme incubation period of several types of PET material. This includes PET from commercial packaging material [48], extruded PET made from recycled PET flakes [84], and amorphous PET samples which have been thermally annealed [28]. This phenomenon has previously been described as a lag phase, and is a result of the random type degradation pattern, as the probability of a chain scissoring near the chain end, resulting in the formation of a soluble product, is inversely proportional with the polymeric chain length of the surface exposed PET chains [85,86].

The duration of these lag phases was shown to depend on the specific surface area of the substrate [84], the X_C [28], and in particular with the enzyme catalyzing the reaction [85]. Notably, higher X_C resulted in extended lag phases. During enzymatic treatment of different low crystalline PET samples ($X_C < 4\%$) from packaging material, a lag phase was observed only on three of these samples (sample no. 29, 38, and 43 from [48]). This observation could therefore indicate that the duration of the lag phases may be affected by other uncharacterized properties of

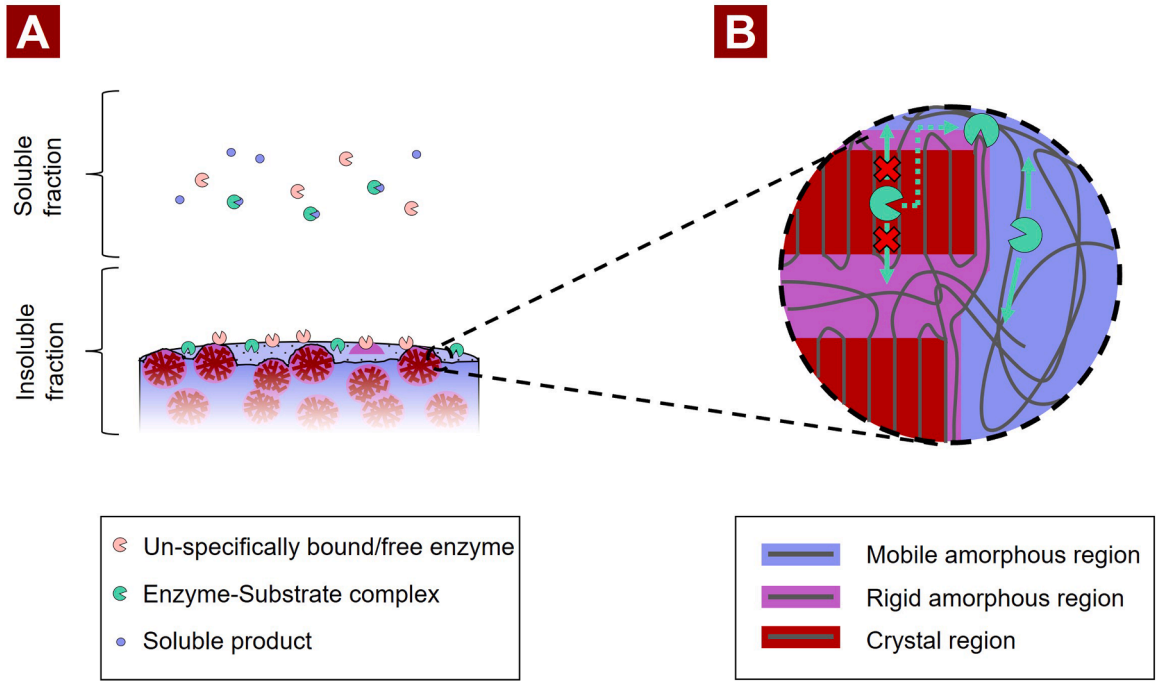

Fig. 4. Schematic representation of the hypothesized enzymatic degradation mechanism of semi-crystalline PET. A) Proposed distribution of enzymes during enzymatic degradation of PET. The enzymes in the soluble fraction may either be unbound free enzyme or bound in an enzyme-substrate complex to soluble hydrolysis products resulting from the enzymatic degradation of PET. The interfacial enzymes bound to the insoluble substrates may either be productive (resulting in hydrolysis) or unproductive. B) Schematic representation of the currently presumed enzymatic attack restrictions in response to the crystallinity features of semi-crystalline PET,
adapted from [83].

the PET material than the X_C. A deeper insight into the causes of the lag phase would enlighten the exact degradation mechanism of PET degrading enzymes. This could furthermore unravel potential synergies between PET degrading enzymes, as both the duration of the lag phase and the steady state reaction rate vary from enzyme to enzyme [85].

Surface modification caused by enzymatic treatment of PET

Evidently, the enzymatic degradation of insoluble PET takes place at the interface of the substrate and the reaction medium. The enzymatic treatment of PET is therefore associated with a change in surface topology of the PET substrate as the reaction progresses. The resulting surface topology, is heavily dependent on the enzyme, the extent of reaction, and the X_C of the PET substrate [28,85]. In addition, Wei et al. [83] showed that the topology of two different postconsumer PET samples with similar X_C was significantly different when degraded by the same enzyme despite an equal extent of reaction. This difference was likely attributed to differences in surface properties of the PET samples (i.e., surface X_C).

The changes in surface topology of an amorphous PET sample resulting from the enzymatic degradation by different enzymes have recently been studied using two of the most promising wild type PET hydrolases, PHL7/PES-H1 (there is currently no consensus on the naming of this enzyme) and LCC [87–89]. These studies showed that the enzymatic degradation of PET resulted in the formation of small shallow pits at the surface of PET samples, and the pits increased in diameter with increasing exposure time [87]. Subsequently new pits were originating within the existing pits, and ultimately replenishing these [88]. This degradation pattern would eventually reach a "steady-state", at which the decrease in the PET film thickness would appear as a uniform degradation [89]. A similar observation was shown on amorphous PET film treated by LCC_{ICCG} [28] – the LCC_{ICCG} being the protein engineered, thermostable gold standard enzyme for PET degradation [90]. The surface erosion caused by enzymatic action on more crystalline PET samples (X_C 15–27%), induced via thermal annealing, were also studied by scanning electron microscopy. These studies of the enzymatic surface erosion revealed that certain areas seemed left "untouched" during the enzymatic degradation. Under the microscope these regions appeared as smooth, flat surface regions within the porous pattern that developed progressively to produce a gradually finer erosion pattern as the enzymatic treatment progressed (Fig. 5). As the X_C increased the size of the porous structures seemed to increase as well [28]. The "untouched" structures were presumably associated with crystal structures resulting from the thermal annealing, as they were not observed on the samples with a lower X_C (<15%) [28]. Prolonged annealing of these samples did, furthermore, result in the exposure of larger crystal structures [85] as shown in Fig. 6B. Interestingly, the surface erosion brought about by PHL7/PES-H1 action resulted in large crater formations, rather than the porous structures obtained by LCC_{ICCG}, these differences were partly attributed to differences in the electrostatic surface potential of the enzymes with PHL7/PES-H1 having a more negative electrostatic potential located on the rear side of the active site. This negative surface potential is proposed to restrict rotation of the PHL7/PES-H1 enzymes once near the negative charges of the carboxylic groups of the hydrolyzed PET, inducing a charge-repulsion that leads to a pseudo-processive function of PHL7/PES-H1 [85]. This is opposite to LCC_{ICCG} which is degrading PET in a true endo-acting manner, thus producing a more uniform degradation pattern across the surface [85].

Effect of X_C on enzymatic degradation of PET

Several engineered enzyme variants originating from different wild type scaffolds have recently been shown capable of achieving depolymerization rates which are relevant for industrial scale degradation of PET. These enzymes include HotPETase (IsPETase backbone), $PES\text{-}H1_{L92F/Q94Y}$, and LCC_{ICCG}, of which the latter, as already mentioned above, is considered the likeliest gold standard candidate, reaching 98% depolymerization within 24 h at industrially relevant conditions [90]. The activity of PET degrading enzymes is, as previously mentioned, highly affected by the X_C of the PET substrate. Several studies have shown how the enzymatic hydrolysis of PET samples with a high X_C is very limited compared to amorphous or low X_C samples [26,27,83,91]. The same trend was observed on commercial PET bottles, as the activity on the more crystalline regions (e.g. body) was significantly lower than the less crystal regions (e.g. the finish/neck) [48,92]. Thermally induced crystallization has been used to quantify the effect of the X_C on the activity of PET hydrolases. This includes both iso-thermal [28] and non-isothermal crystallization [93]. Here both studies showed that the activity is affected in a non-linear matter, and that activity is almost depleted at $X_C > 17–20\%$. The X_C determined in both studies were measured by Differential Scanning Calorimetry (DSC), and the X_C therefore reflects the bulk X_C rather than the X_C at the surface exposed to the enzymes. This issue of X_C determination is discussed further in a later section.

A recent comparative assessment of six thermostable PET hydrolases performed by the authors of this paper reviled that this threshold varied between the enzymes [85]. For a quantitative assessment of this phenomenon, we defined the term tolerance, which corresponds to the X_C at which the residual activity is 50% of what was obtained on a PET sample of very low X_C. The tolerance to X_C of the six thermostable enzymes examined is summarized in the upper part of Table 1.

Despite this, it has been shown that PET particles at higher X_C values (>30%) was amendable to enzymatic hydrolysis [59,94–96]. The overall extent of reaction was, however, lower compared to substrate at

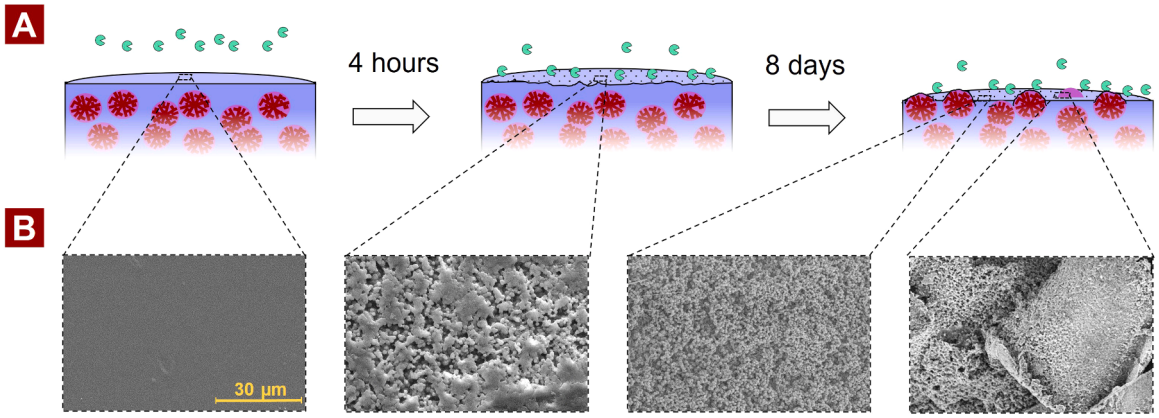

Fig. 5. Change in surface topology during enzymatic degradation of semi-crystalline PET. A) Schematic representation of the surface erosion of a PET film caused by enzymatic treatment. B) SEM images of the surface erosion caused by enzymatic treatment of annealed PET disk (X_C = 23.3%) using LCC_{ICCG} adapted from [28,85].

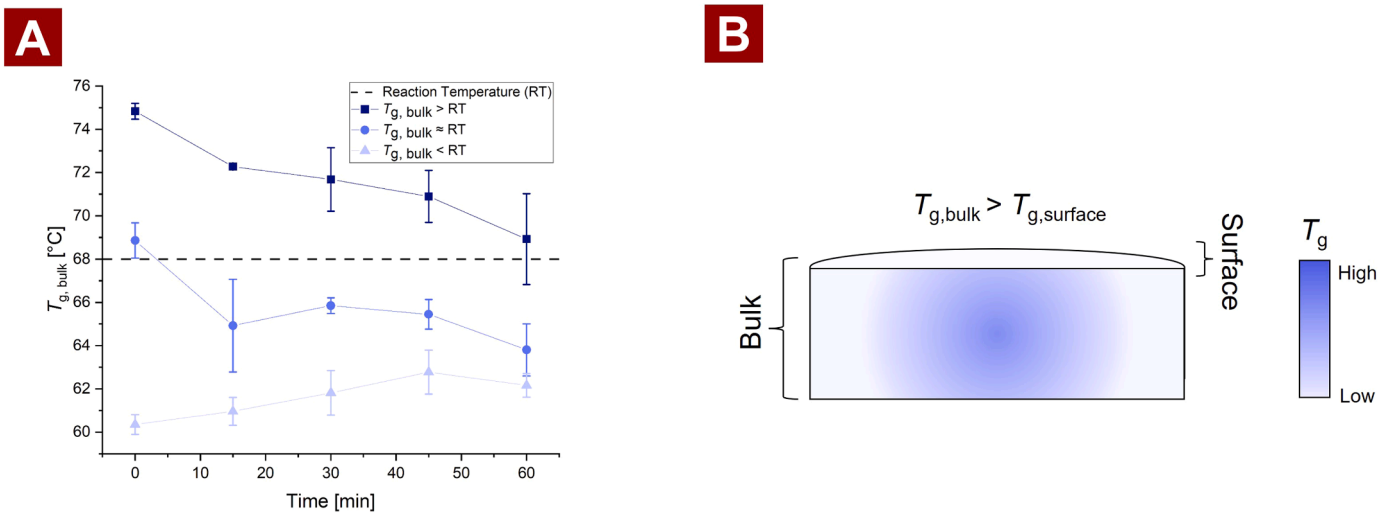

Fig. 6. A) Change in T_g during 1 h of incubation with LCC_{ICCG} at 68 °C [28]. B) Schematic representation of the T_g gradient trend in a PET sample.

Table 1
List of enzymes that have been characterized in terms of their tolerance to PET crystallinity. A. Direct tolerance to X_C as threshold when activity was halved[a]; B. Relative ratio, termed selectivity ratio, between the activity on amorphous (X_C 6.2%) and highly crystalline PET (X_C 39.3%).

A. Assessment of tolerance, adapted from [85]			
Enzyme	Origin (Phylum)	EC number	Tolerance (% X_C)[a]
LCC (sp|G9BY57|)	Actinobacteriota	3.1.1.74	23.2 ± 2.6
LCC_{ICCG} (sp|G9BY57|)	Actinobacteriota	3.1.1.74	20.9 ± 2.1
DuraPETase (sp|A0A0K8P6T7|)	Pseudomonadota	3.1.1.101	17.1 ± 0.9
PHL7/PES-H1 (pdb|7NEI/7CUV|)	-	3.1.1.74	17.4 ± 1.9
TfC (AJ810119.1)	Actinobacteriota	3.1.1.74	14.3 ± 0.8
HiC (tr|A0A075B5G4|)	Eukarya	3.1.1.74	13.7 ± 0.5
B. Relative product formation on crystalline PET powder vs on amorphous film, from [98]			
Enzyme	Origin (Phylum)	EC number	Selectivity ratio[b]
LCC_{ICCG} (sp|G9BY57|)	Actinobacteriota	3.1.1.74	0.19
503 (EGD44994.1)	Actinobacteriota	-	1.30
602/Tcur0390 (ACY95991.1)	Actinobacteriota	3.1.1.74	2.79
711/est119 (sp|F7IX06|)	Actinobacteriota	3.1.1.1	2.13

[a] Calculated at the X_C (%) at which the reaction rate was half the of the rate obtained on amorphous PET (X_C = 10.8%) [85];
[b] Calculated as the ratio between the activity of the enzyme on crystalline PET powder (X_C = 39.3%) divided by the activity on amorphous powder (X_C = 6.2%) according to [98].

lower X_C [59,95], and may be explained by the disproportionally large surface area of the small substrate particles.

Brizendine et. al recently studied the effect of particle size on the degradation of highly crystalline PET (32.5–35.7% X_C) and Cryo-grinded PET particles (7–15% X_C). This study revealed that the reaction rate increased with the specific surface area , while the overall extent of reaction was unaffected by the particle size [95]. Kaabel et. al showed that the extent of reaction could be improved via a mechano-enzymatic hydrolysis (ball milling followed by an enzymatic treatment at 55 °C) of a PET powder slurry [96]. Here, nearly 50% yield of TPA was reached after 21 cycles in their process. Another attempt to increase the efficiency of PET degrading enzymes towards the crystalline regions was made by improving the selectivity towards the *trans* confirmation [97]. This improvement was achieved by engineering an *Is*PETase via rational design assisted by MD simulation and molecular docking [97]. The S238A variant showed a 2.8-fold higher activity on a *trans*-enriched PET oligomeric substrate, obtained through a microwave-pretreatment, compared to the wildtype. As the average chain length of the *trans*-enriched PET corresponded to smaller oligomers, the result may not reflect the degradation of all-trans crystal lamella or trans rich RAF found in untreated semi-crystalline PET [97]. The selectivity towards the crystalline regions has also been assessed through a comparative evaluation of 51 putative PET hydrolases from 7 district phylogenetic groups [98]. Here three enzymes displayed a higher activity on crystalline PET powder compared to amorphous PET powder. These three enzymes 503, 602, and 711 are highlighted in Table 1.

As pointed out in this review, currently a main limitation of biocatalytic recycling of plastics is the limited activity of the currently characterized PET degrading enzymes on PET of relevant crystallinity, i.e., X_C> ~20% (Table 1) [27,28,48,83]. A pre-treatment step involving extrusion and micronization is therefore currently required as pre-treatment to accomplish efficient enzymatic degradation of PET [27]. An impact analysis of the enzymatic recycling of PET has pointed out that the elimination of the pretreatment step would decrease the minimal selling price of the degradation products by 12% and reduce its greenhouse gas emission by 38% [30]. This is under the assumption that the catalytic efficiency of the enzymes remains unchanged.

Effect of T_g on enzymatic degradation of PET

Water may act as a plasticizer PET, and a decrease in T_g of PET material is therefore expected during enzymatic treatment, as these reactions are performed in aqueous solutions. We recently investigated the effect of decreased T_g values of PET on enzymatic degradation efficiency [59]: By soaking a PET sample in water for 24 h at 65 °C, the T_g was

Table 2
Change in T_g and X_C during the enzymatic treatment of PET disks using LCC_{ICCG} at pH 9 and a temperature of reaction (TR) of 68 °C. Disks were subjected to different soaking conditions to achieve distinct starting T_g values. The reaction rate was assessed for each substrate with $T_{g,\ bulk} > TR$, $T_{g,\ bulk} \approx TR$, and $T_{g,\ bulk} < TR$. The data presented in the table are adapted from [28].

	Soaking condition	$T_{g,bulk\ start}$ [°C]	$T_{g,bulk\ final}$ [°C]	$X_{C\ start}$ [%]	$X_{C\ final}$ [%]	Rate [mM/h]
$T_{g,\ bulk} > TR$	n/a	74.8 ± 0.4^a	68.8 ± 2.1^a	11.2 ± 1.0^a	10.9 ± 1.5^a	4.81 ± 0.83^a
$T_{g,\ bulk} \approx TR$	24 h, 45 °C	68.9 ± 0.8^b	63.8 ± 1.2^b	11.5 ± 1.1^a	10.7 ± 0.9^a	4.56 ± 0.64^a
$T_{g,\ bulk} < TR$	24 h, 65 °C	60.4 ± 0.5^c	62.2 ± 0.5^b	11.7 ± 0.2^a	11.2 ± 0.6^a	4.38 ± 0.86^a

[a,b,c] Different roman superscript letters, a-c, within the same column indicate significantly different values ($p < 0.05$).

lowered from 75 °C to 61 °C, without affecting the X_C. The activity of the thermostable LCC variant, LCC_{ICCG}, was measured on both the untreated (T_g = 75 °C) and the soaked (T_g = 61 °C) PET samples (sheets), at a reaction temperature between the T_g value of the two samples (68 °C). It would be expected that the mobility of the PET chains in the soaked sample would be greater when the reaction temperature was above the T_g (Fig. 6A). However, the activity of the LCC_{ICCG} enzyme was, not affected by the decreased T_g [59] (Fig. 6B. Table 2).

The T_g- and X_C-values from the abovementioned study were measured using DSC and therefore reflects the bulk rather than the surface. In fact, as previously indicated, it has been shown the T_g at the surface of PET is usually substantially lower than the T_g of bulk PET (as low as 40 °C) [86,99–101]. Consequently, the local T_g of a thicker PET sample would gradually increase from the surface into the bulk of the samples, as illustrated in Fig. 6. An increase in the mobility of the surface exposed polymeric chains is therefore expected to occur at temperatures much lower than the bulk T_g of the PET material [86]. These results indicate that the increase in activity at temperatures near the bulk T_g is mainly driven by the thermal activation of enzyme activity (k_{cat}), rather than by increased chain mobility of the substrate resulting from devitrification (provided the enzyme is sufficiently thermostable).

The lower T_g at the surface of a PET material also explains the on-set temperatures of surface and bulk crystals, as crystallization may only occur at the surface when the temperature is below the bulk T_g and above the surface T_g. The decreasing T_g at the surface is however suppressed by the RAF associated with the increase in X_C resulting from the formation of surface crystals [101]. It is therefore not suitable to run reaction at 70 °C or above, as the crystallization, and thus increase in X_C, occurring at these high temperatures lowers the reaction rate of the enzyme [27]. The optimal reaction temperature of the enzymatic degradation of PET may therefore be governed by the crystallization of the substrate rather than by thermal inactivation of the enzyme [28].

The complexity of the T_g effect, leading to increased substrate mobility upon devitrification, versus the direct enhanced enzymatic reaction rate effect, i.e., the Arrhenius effect, is corroborated by the findings that the activity of PET hydrolases increases drastically in the temperature range from 50 °C to 70 °C on a low X_C PET film, compared to on a highly crystalline PET powder [102]. The same is found on poly (vinyl acetate), which has a lower T_g of 32 °C [37,103]. It is tempting to infer that these findings are a result of the MAF of amorphous PET film undergoing transition to its more mobile state during this temperature interval. Such transition has been shown to occur at temperatures as low as 40 °C [86]. However, this explanation does not hold for a crystalline sample, as it presumably has a limited content of MAF. Similarly, no transition occurs for poly(vinyl acetate), as it devitrifies at lower temperatures than PET [103].

Due to the complexity of the PET substrate as highlighted in this review it is evident that other, yet uncharacterized factors may also affect the enzymatic degradation PET. This includes the change in surface electrostatics at the surface of PET caused by the exposure of two acid groups, when a PET chain is hydrolyzed in an endo-type manner [77,85]. Moreover, the extent of entanglement could potentially affect the enzymatic degradation of PET. To the best of our knowledge, this aspect has not yet been studied in relation to the enzymatic hydrolysis of PET. Nevertheless, we speculate that the greater presence of entanglements could hinder sterically the accessibility of the most hydrolysable regions of the PET substrate via the entanglements blocking the formation of an enzyme-substrate complex. It could therefore be relevant to quantify how the extent of entanglement, quantified in terms of MW_e, which is, as previously mentioned, a quantitative measure of the average distance between chain entanglements within the PET substrate.

Current limitations of existing methodologies

The majority of previous studies investigating on the effect of crystallinity on the enzymatic degradation of PET has been carried out by comparing the activity on PET substrates processed in various manners, such as amorphous PET film and crystalline PET powder [26,37,97,98,102,104–106]. This approach is not ideal because these substrates may vary in other properties, like the specific surface area and crystal morphology, which can also influence the enzymatic hydrolysis rate itself [83,84,95], thus introducing a bias into the results, as observed changes in the rate may be caused by other factors than the X_C only.

The X_C and T_g of measurement of PET samples used in enzyme assays are most commonly quantified by DSC [26,28,37,83,85,93,95,98,102,104–106]. However, there are precautions associated with the interpretation of DSC measurements for characterizing PET intended for enzymatic degradation. One major issue is that the calculated values represent an average of the entire sample (bulk). The bulk values might not represent the X_C at the surface, which would be the case for PET samples with surface crystals which are formed at lower temperatures [51], an issue which is of particular significance since the enzymatic degradation of PET is an interfacial process. In addition, the bulk T_g of PET is, as previously mentioned, lower than the T_g at the surface [99–101]. The DSC measurements of the T_g and X_C values are furthermore affected by the heating rate [44]. DSC measures should always be performed at the same heating rate, i.e., at 10 °C/min for direct comparison between studies [59]. Alternatively, the heat rate independent T_g-value, $T_{g(0)}$, can calculated by extrapolating the T_g obtained at different heating rates [107]. This approach may give a more accurate measurement of the actual T_g of the bulk PET: $T_{g(0)}$ was found to be ca. 65 °C for amorphous PET [108]. Therefore, standardized analysis methods for quantifying the surface X_C and T_g of PET should be implemented when studying the effect of substrate properties on PET degrading enzymes. Such an approach could involve infrared spectroscopy measurements in addition to DSC measurements. In fact, it has previously been shown that change in peak intensity from attenuated total reflectance Fourier transform infrared (ATR-FTIR) spectroscopy correlates with X_{MAF} [59]. Additionally, a standardized set of PET substrates of different levels of known X_C, is required to quantitatively characterize the action kinetics of PET degrading enzymes [59,109]. As highlighted in a recent paper by Arnal et al. [90] it is furthermore important to develop a consensus of the parameters used for the evaluation of the performance of PET degradation enzymes. These should not be limited to the specific activity at a certain condition, but also include the total depolymerization yield (in terms of TPA and EG conversion).

Conclusions and future trends

The fractional composition of PET as a substrate for biorecycling, especially the relative level of crystalline regions, i.e., the degree of crystallinity, X_C, strongly affects the activity of PET degrading enzymes. When the X_C exceeds ~20% [28,93], the activity of the currently known PET degrading enzymes such as LCC_{ICCG}, DuraPETase, and PHL7/PES-H1, is limited - if not completely abolished - which is a major challenge for enzymatic recycling of PET, as most waste PET, notably the PET constituting the major part of plastic bottles, is highly crystalline (X_C>25%) [48]. Such high crystallinity is a result of the thermo-mechanical molding process of the PET polymer resin to the desired shape at high temperature because crystals form during the slow cooling from temperatures above the T_g of PET, and because of stretching of the hot material at temperatures above the T_g - the latter phenomenon being referred to as strain induced crystallization.

In the budding industrial enzyme based recycling of PET bottles, a pretreatment step is therefore used to make the substrate more amorphous and thus amendable to enzymatic degradation [30,110]. This pretreatment is, however, undesirable as it is highly energy demanding. To achieve as enzymatic high turnover rates (k_{cat}) as possible, industrial enzymatic reactions are to be run at as high temperatures as possible, to enable a thermal rate activation of the enzyme and to facilitate the transition of the mobile amorphous PET chains into their more mobile state. This transition occurs at the T_g of the material. However, it has been observed that this transition occurs at temperatures considerably lower than the T_g of the bulk material, particularly at the surface in an aqueous environment (40 °C) [86]. Although highly thermostable PET degrading enzymes have now been developed by protein engineering, the nature of the thermal crystallization of PET dictates that the maximal reaction temperature of the enzymatic processing step is max. 65–68 °C, as reaction above ~70 °C, which is significantly below the T_m of current PET degrading enzymes [27], reduces reaction rate and hydrolysis yield of the enzymes [27,28].

Recently EU has passed legislation requiring that a tax of EUR 0.80 per kilo be imposed on newly produced plastics - i.e. plastics which are not made from recycled plastics [111]. This is equivalent to approximately 100–160% of the costs of the precursors used for the molding of new PET products [30] and is expected to have a positive impact on the recycling of plastics, and further fuel the enzymatic recycling of plastics as a sustainable technology option. For this to be successful, a better understanding of the degradation mechanism of PET degrading enzymes on semi-crystalline PET of $X_C > 20\%$ is therefore required to determine how the activity against the crystalline regions PET can be improved. This can only be achieved by directing the research within the field of plastic degrading enzymes into the characterization of substrate and enzyme interactions.

We anticipate that the next important step forward in advancing the field of enzymatic PET degradation and recycling is to develop a deeper understanding of the significance of the PET as a semi-crystalline enzyme substrate. More specifically the catalytic interactions between the enzyme and the microstructures of PET (represented by X_C, X_{RAF}, and X_{MAF}), and how this interaction is affected by the water-induced plasticization of the surface exposed polymer chains of PET, and how these features change during the dynamic enzymatic degradation of PET. Even though water diffusion into PET is profoundly reduced at X_C of 25% [112], this improved understanding would ideally reveal the features required for efficient degradation of PET with X_C above 20% and allow for rational approaches for selection or development of efficient PET degrading enzymes with activity towards the crystalline regions.

CRediT authorship contribution statement

TBT and ASM: Conceptualization. TBT: Original draft preparation and Visualization. TBT, KA and ASM: Writing, Reviewing, Editing.

Declaration of Competing Interest

The authors declare that they have no known competing financial interests or personal relationships that could have appeared to influence the work reported in this paper. All authors are employed at the Technical University of Denmark.

Data Availability

It is a review paper, that builds on avaialble data.

Acknowledgements

Financial support from The Villum Experiment Programme, VIL-Grant no. 40815, is highly acknowledged.

References

[1] Geyer R, Jambeck JR, Law KL. Production, use, and fate of all plastics ever made. Sci Adv 2017;3:e1700782. https://doi.org/10.1126/sciadv.1700782.
[2] European Commission. A circular economy for plastics – Insights from research and innovation to inform policy and funding decisions. 2019. https://doi.org/10.2777/269031.
[3] Plastics Europe. Plastics – the Facts 2022. Available at: https://Plasticseurope.Org/Knowledge-Hub/Plastics-the-Facts-2022/: 2022.
[4] Textile Exchange. Preferred Fiber & Materials Market Report 2021. Available at: https://Textileexchange.Org/Knowledge-Center/Reports/Preferred-Fiber-Materials-Market-Report-2021//: 2021.
[5] Ingrao C, Wojnarowska M. Findings from a streamlined life cycle assessment of PET-bottles for beverage-packaging applications, in the context of circular economy. Sci Total Environ 2023;892:164805. https://doi.org/10.1016/j.scitotenv.2023.164805.
[6] World Economic Forum Ellen MacArthur Foundation McKinsey & Company. The New Plastics Economy: Rethinking the future of plastics. Available at: https://Ellenmacarthurfoundation.Org/the-New-Plastics-Economy-Rethinking-the-Future-of-Plastics: 2016.
[7] Barnes DKA, Galgani F, Thompson RC, Barlaz M. Accumulation and fragmentation of plastic debris in global environments. Philos Trans R Soc B Biol Sci 2009;364:1985–98. https://doi.org/10.1098/rstb.2008.0205.
[8] Knoblauch D, Mederake L. Government policies combatting plastic pollution. Curr Opin Toxicol 2021;28:87–96. https://doi.org/10.1016/j.cotox.2021.10.003.
[9] Nielsen TD, Hasselbalch J, Holmberg K, Stripple J. Politics and the plastic crisis: A review throughout the plastic life cycle. Wiley Inter Rev Energy Environ 2020;9:e360. https://doi.org/10.1002/wene.360.
[10] European Council. Directive (Eu) 2019/904 of the European Parliament and of the Council of 5 June 2019 on the reduction of the impact of certain plastic products on the environment. Available at: https://Eur-Lex.Europa.Eu/Legal-Content/EN/ALL/?Uri=LEGISSUM%3A4393034: 2019.
[11] Ellen McArthur Foundation, UNEP. The Global Commitment 2022 Progress Report. 2022. Available at: https://www.ellenmacarthurfoundation.org/global-commitment-2022/overview.
[12] Unesda, Natural Mineral Waters Europe, Petcore Europe. The PET market in Europe. State of Play 2002. Available at: https://www.unesda.eu/wp-content/uploads/2022/01/PET-Market-in-Europe-State-of-Play-2022.pdf.
[13] Luo ZW, Lee SY. Biotransformation of p-xylene into terephthalic acid by engineered *Escherichia coli*. Nat Commun 2017;8:1–8. https://doi.org/10.1038/ncomms15689.
[14] Aharoni SM. Industrial-scale production of polyesters, especially poly(ethylene terephthalate). In: Fakirov S, editor. Handbook of Thermoplast. Polyesters. Wiley-VCH; 2002. p. 59–103. https://doi.org/10.1002/3527601961.ch2.
[15] Schyns ZOG, Shaver MP. Mechanical recycling of packaging plastics: a review. Macromol Rapid Commun 2021;42:1–27. https://doi.org/10.1002/marc.202000415.
[16] Badia JD, Strömberg E, Karlsson S, Ribes-Greus A. The role of crystalline, mobile amorphous and rigid amorphous fractions in the performance of recycled poly (ethylene terephthalate) (PET). Polym Degrad Stab 2012;97:98–107. https://doi.org/10.1016/J.POLYMDEGRADSTAB.2011.10.008.
[17] Ragaert K, Delva L, Van Geem K. Mechanical and chemical recycling of solid plastic waste. Waste Manag 2017;69:24–58. https://doi.org/10.1016/j.wasman.2017.07.044.
[18] Torres N, Robin JJ, Boutevin B. Study of thermal and mechanical properties of virgin and recycled poly(ethylene terephthalate) before and after injection molding. Eur Polym J 2000;36:2075–80. https://doi.org/10.1016/S0014-3057(99)00301-8.
[19] Jönsson C, Wei R, Biundo A, Landberg J, Schwarz Bour L, Pezzotti F, et al. Biocatalysis in the recycling landscape for synthetic polymers and plastics towards circular textiles. ChemSusChem 2021;14:4028–40. https://doi.org/10.1002/cssc.202002666.
[20] Geyer R, Kuczenski B, Zink T, Henderson A. Common misconceptions about recycling. J Ind Ecol 2016;20:1010–7. https://doi.org/10.1111/jiec.12355.

[21] Marten E, Müller RJ, Deckwer WD. Studies on the enzymatic hydrolysis of polyesters. II. Aliphatic-aromatic copolyesters. Polym Degrad Stab 2005;88:371–81. https://doi.org/10.1016/j.polymdegradstab.2004.12.001.

[22] Müller RJ, Schrader H, Profe J, Dresler K, Deckwer WD. Enzymatic degradation of poly(ethylene terephthalate): Rapid hydrolyse using a hydrolase from *T. fusca*. Macromol Rapid Commun 2005;26:1400–5. https://doi.org/10.1002/marc.200500410.

[23] Yoshida S, Hiraga K, Takehana T, Taniguchi I, Yamaji H, Maeda Y, et al. A bacterium that degrades and assimilates poly(ethylene terephthalate. Science 2016;351:1196–9. https://doi.org/10.1126/science.aad6359.

[24] Wei R, Von Haugwitz G, Pfaff L, Mican J, Badenhorst CPS, Liu W, et al. Mechanism-based design of efficient PET hydrolases. ACS Catal 2022;12:3382–96. https://doi.org/10.1021/acscatal.1c05856.

[25] Quartinello F, Vajnhandl S, Volmajer Valh J, Farmer TJ, Vončina B, Lobnik A, et al. Synergistic chemo-enzymatic hydrolysis of poly(ethylene terephthalate) from textile waste. Micro Biotechnol 2017;10:1376–83. https://doi.org/10.1111/1751-7915.12734.

[26] Vertommen MAME, Nierstrasz VA, Veer MVan Der, Warmoeskerken MMCG. Enzymatic surface modification of poly(ethylene terephthalate). J Biotechnol 2005;120:376–86. https://doi.org/10.1016/j.jbiotec.2005.06.015.

[27] Tournier V, Topham CM, Gilles A, David B, Folgoas C, Moya-Leclair E, et al. An engineered PET depolymerase to break down and recycle plastic bottles. Nature 2020;580:216–9. https://doi.org/10.1038/s41586-020-2149-4.

[28] Thomsen TB, Hunt CJ, Meyer AS. Influence of substrate crystallinity and glass transition temperature on enzymatic degradation of polyethylene terephthalate (PET). N Biotechnol 2022;69:28–35. https://doi.org/10.1016/j.nbt.2022.02.006.

[29] Zimmermann W. Biocatalytic recycling of polyethylene terephthalate plastic. Philos Trans R Soc A 2020:378. https://doi.org/10.1098/RSTA.2019.0273.

[30] Singh A, Rorrer NA, Nicholson SR, Erickson E, DesVeaux JS, Avelino AFT, et al. Techno-economic, life-cycle, and socioeconomic impact analysis of enzymatic recycling of poly(ethylene terephthalate). Joule 2021. https://doi.org/10.1016/j.joule.2021.06.015.

[31] Tiso T, Narancic T, Wei R, Pollet E, Beagan N, Schröder K, et al. Towards bio-upcycling of polyethylene terephthalate. Metab Eng 2021;66:167–78. https://doi.org/10.1016/j.ymben.2021.03.011.

[32] Zumstein MT, Rechsteiner D, Roduner N, Perz V, Ribitsch D, Guebitz GM, et al. Enzymatic hydrolysis of polyester thin films at the nanoscale: effects of polyester structure and enzyme active-site accessibility. Environ Sci Technol 2017;51:7476–85. https://doi.org/10.1021/ACS.EST.7B01330.

[33] Tokiwa Y, Suzuki T. Hydrolysis of polyesters by lipases. Nature 1977;270:76–8. https://doi.org/10.1038/270076a0.

[34] Wei R, Zimmermann W. Microbial enzymes for the recycling of recalcitrant petroleum-based plastics: how far are we? Micro Biotechnol 2017;10:1308–22. https://doi.org/10.1111/1751-7915.12710.

[35] IUBMB. IUBMB Nomenclature Home Page 2016. https://iubmb.qmul.ac.uk/enzyme/EC3/0101b.html#101 (Accessed 10 August 2023).

[36] Sulaiman S, You DJ, Kanaya E, Koga Y, Kanaya S. Crystal structure and thermodynamic and kinetic stability of metagenome-derived LC-cutinase. Biochemistry 2014;53:1858–69. https://doi.org/10.1021/bi401561p.

[37] Ronkvist ÅM, Xie W, Lu W, Gross RA. Cutinase-catalyzed hydrolysis of poly(ethylene terephthalate. Macromolecules 2009;42:5128–38. https://doi.org/10.1021/ma9005318.

[38] Kawai F. The current state of research on PET hydrolyzing enzymes available for biorecycling. Catalysts 2021;11:1–10. https://doi.org/10.3390/catal11020206.

[39] Buchholz PCF, Feuerriegel G, Zhang H, Perez-Garcia P, Nover L-L, Chow J, et al. Plastics degradation by hydrolytic enzymes: The plastics-active enzymes database—PAZy. Proteins 2022;90:1443–56. https://doi.org/10.1002/PROT.26325.

[40] Haernvall K, Zitzenbacher S, Yamamoto M, Schick MB, Ribitsch D, Guebitz GM. A new arylesterase from *Pseudomonas pseudoalcaligenes* can hydrolyze ionic phthalic polyesters. J Biotechnol 2017;257:70–7. https://doi.org/10.1016/j.jbiotec.2017.01.012.

[41] Gambarini V, Pantos O, Kingsbury JM, Weaver L, Handley KM, Lear G. PlasticDB: a database of microorganisms and proteins linked to plastic biodegradation. Database 2022;2022:baac008. https://doi.org/10.1093/database/baac008.

[42] Gan Z, Zhang H. PMBD: a comprehensive plastics microbial biodegradation database. Database 2019;2019:baz119. https://doi.org/10.1093/database/baz119.

[43] Jog JP. Crystallization of polyethyleneterephthalate. J Macromol Sci Part C 1995;35:531–53. https://doi.org/10.1080/15321799508014598.

[44] Wellen RMR, Canedo E, Rabello MS. Nonisothermal cold crystallization of poly(ethylene terephthalate). J Mater Res 2011;26:1107–15. https://doi.org/10.1557/jmr.2011.44.

[45] Bartczak Z. Deformation of semicrystalline polymers – the contribution of crystalline and amorphous phases. Polimery 2017;62:787–99. https://doi.org/10.14314/POLIMERY.2017.787.

[46] Webb HK, Arnott J, Crawford RJ, Ivanova EP. Plastic degradation and its environmental implications with special reference to poly(ethylene terephthalate. Polym (Basel) 2013;5:1–18. https://doi.org/10.3390/polym5010001.

[47] Karacan I. An in depth study of crystallinity, crystallite size and orientation measurements of a selection of poly(ethylene terephthalate) fibers. Fibers Polym 2005;6:186–99.

[48] Lu H, Diaz DJ, Czarnecki NJ, Zhu C, Kim W, Shroff R, et al. Machine learning-aided engineering of hydrolases for PET depolymerization. Nature 2022;604:662–7. https://doi.org/10.1038/s41586-022-04599-z.

[49] Zekriardehani S, Jabarin SA, Gidley DR, Coleman MR. Effect of chain dynamics, crystallinity, and free volume on the barrier properties of poly(ethylene terephthalate) biaxially oriented films. Macromolecules 2017;50:2845–55. https://doi.org/10.1021/acs.macromol.7b00198.

[50] Mandal S, Dey A. PET Chemistry. In: Thomas S, Kanny K, Thomas MG, editors. Recycling of Polyethyl Terephthalate Bottles. Elsevier; 2019. p. 1–22. https://doi.org/10.1016/b978-0-12-811361-5.00001-8.

[51] Shinotsuka K, Assender H. In situ AFM study of near-surface crystallization in PET and PEN. J Appl Polym Sci 2016;133:44269. https://doi.org/10.1002/app.44269.

[52] Jabarin SA. Crystallization kinetics of poly(ethylene terephthalate). III. Effect of moisture on the crystallization behavior of PET from the glassy state. J Appl Polym Sci 1987;34:103–8. https://doi.org/10.1002/APP.1987.070340109.

[53] Baldenegro-Perez LA, Navarro-Rodriguez D, Medellin-Rodriguez FJ, Hsiao B, Avila-Orta CA, Sics I. Molecular weight and crystallization temperature effects on poly(ethylene terephthalate) (PET) homopolymers, an isothermal crystallization analysis. Polym (Basel) 2014;6:583–600. https://doi.org/10.3390/polym6020583.

[54] Llana PG, Boyce MC. Finite strain behavior of poly(ethylene terephthalate) above the glass transition temperature. Polym (Guildf) 1999;40:6729–51. https://doi.org/10.1016/S0032-3861(98)00867-2.

[55] Demirel B, Yaraş A, Elçiçek H. Crystallization Behavior of PET Materials. BAÜ Fen Bil Enst Derg Cilt 2011;13:26–35.

[56] Gorlier E, Haudin JM, Billon N. Strain-induced crystallisation in bulk amorphous PET under uni-axial loading. Polym (Guildf) 2001;42:9541–9. https://doi.org/10.1016/S0032-3861(01)00497-9.

[57] Guo X, Wang J. The chemical behaviors of microplastics in marine environment: a review. Mar Pollut Bull 2019;142:1–14. https://doi.org/10.1016/j.marpolbul.2019.03.019.

[58] Kurita T, Fukuda Y, Takahashi M, Sasanuma Y. Crystalline moduli of polymers, evaluated from density functional theory calculations under periodic boundary conditions. ACS Omega 2018;3:4824–35. https://doi.org/10.1021/acsomega.8b00506.

[59] Thomsen TB, Hunt CJ, Meyer AS. Standardized method for controlled modification of poly (ethylene terephthalate) (PET) crystallinity for assaying PET degrading enzymes. MethodsX 2022;9:101815. https://doi.org/10.1016/J.MEX.2022.101815.

[60] Karagiannidis PG, Stergiou AC, Karayannidis GP. Study of crystallinity and thermomechanical analysis of annealed poly(ethylene terephthalate) films. Eur Polym J 2008;44:1475–86. https://doi.org/10.1016/j.eurpolymj.2008.02.024.

[61] Liu J, Geil PH. Crystal structure and morphology of poly(ethylene terephthalate) single crystals prepared by melt polymerization. J Macromol Sci - Phys 1997;36:61–85. https://doi.org/10.1080/00222349708220415.

[62] Hu W, Zha L. Theoretical aspects of polymer crystallization. In: Mitchell G, Tojeira A, editors. Controlling the Morphology of Polymers. Springer; 2016. p. 101–43. https://doi.org/10.1007/978-3-319-39322-3_4.

[63] Baldenegro-Perez LA, Navarro-Rodriguez D, Medellin-Rodriguez FJ, Hsiao B, Avila-Orta CA, Sics I. Molecular eeight and crystallization temperature effects on poly(ethylene terephthalate) (PET) homopolymers, an isothermal crystallization analysis. Polym 2014;6:583–600. https://doi.org/10.3390/POLYM6020583.

[64] Li Y, Makita Y, Zhang G, Rui G, Li ZM, Zhong GJ, et al. Effects of rigid amorphous fraction and lamellar crystal orientation on electrical insulation of poly(ethylene terephthalate) films. Macromolecules 2020;53:3967–77. https://doi.org/10.1021/acs.macromol.0c00646.

[65] Lu XF, Hay JN. Isothermal crystallization kinetics and melting behaviour of poly(ethylene tereph-thalate). Polym (Guildf) 2001;42:9423–31. https://doi.org/10.1016/S0032-3861(01)00502-X.

[66] Al Raheil IAM. Morphology and crystallization of poly(ethylene terephthalate). Polym Int 1994;35:189–95. https://doi.org/10.1002/pi.1994.210350209.

[67] Jabarin SA. Strain-induced crystallization of poly(ethylene terephthalate). Polym Eng Sci 1992;32:1341–9. https://doi.org/10.1002/pen.760321802.

[68] Mitchell GR, Tojeira A. Control Morphol Polym: Mult Scales Struct Process 2016. https://doi.org/10.1007/978-3-319-39322-3.

[69] Tsai RS, Lee DK, Fang HY, Tsai HB. Crystalline study of amorphous poly(ethylene terephthalate) sheets through annealing. Asia-Pac J Chem Eng 2009;4:140–6. https://doi.org/10.1002/apj.189.

[70] Cusano I, Campagnolo L, Aurilia M, Costanzo S, Grizzuti N. Rheology of recycled PET. Mater (Basel) 2023;16:1–23. https://doi.org/10.3390/ma16093358.

[71] Androsch R, Wunderlich B. The link between rigid amorphous fraction and crystal perfection in cold-crystallized poly(ethylene terephthalate). Polym (Guildf) 2005;46:12556–66. https://doi.org/10.1016/J.POLYMER.2005.10.099.

[72] Di Lorenzo ML, Righetti MC, Cocca M, Wunderlich B. Coupling between crystal melting and rigid amorphous fraction mobilization in poly(ethylene terephthalate. Macromolecules 2010;43:7689–94. https://doi.org/10.1021/MA101035H.

[73] Slobodian P. Rigid amorphous fraction in poly(ethylene terephthalate) determined by dilatometry. J Therm Anal Calor 2008;94:545–51. https://doi.org/10.1007/s10973-007-8566-x.

[74] Choi J, Cakmak M. Morphological evolution during thermal and strain induced crystallization in poly(ethylene terephthalate)/poly(ether imide) blend films. Polym (Guildf) 2016;84:10–20. https://doi.org/10.1016/J.POLYMER.2015.12.038.

[75] Levine H, Grenet J, Slade L. Water as a plasticizer: physico-chemical aspects of low-moisture polymeric systems. Eur Polym J 1993;30:339–45. https://doi.org/10.1017/cbo9780511552083.002.

[76] Chen Y, Lin Z, Yang S. Plasticization and crystallization of poly(ethylene terephthalate) induced by water. J Therm Anal Calor 1998;52:565–8. https://doi.org/10.1023/A:1010123723719.
[77] Eberl A, Heumann S, Brückner T, Araujo R, Cavaco-Paulo A, Kaufmann F, et al. Enzymatic surface hydrolysis of poly(ethylene terephthalate) and bis (benzoyloxyethyl) terephthalate by lipase and cutinase in the presence of surface active molecules. J Biotechnol 2009;143:207–12. https://doi.org/10.1016/J.JBIOTEC.2009.07.008.
[78] Austin HP, Allen MD, Donohoe BS, Rorrer NA, Kearns FL, Silveira RL, et al. Characterization and engineering of a plastic-degrading aromatic polyesterase. Proc Natl Acad Sci USA 2018;115:E4350–7. https://doi.org/10.1073/pnas.1718804115.
[79] Schubert SW, Schaller K, Bååth JA, Hunt C, Borch K, Jensen K, et al. Reaction pathways for the enzymatic degradation of poly(ethylene terephthalate): What characterizes an efficient PET-hydrolase? ChemBioChem 2022;24:e202200516. https://doi.org/10.1002/CBIC.202200516.
[80] Arnling Bååth J, Novy V, Carneiro LV, Guebitz GM, Olsson L, Westh P, et al. Structure-function analysis of two closely related cutinases from *Thermobifida cellulosilytica*. Biotechnol Bioeng 2022;119:470–81. https://doi.org/10.1002/BIT.27984.
[81] Barth M, Oeser T, Wei R, Then J, Schmidt J, Zimmermann W. Effect of hydrolysis products on the enzymatic degradation of polyethylene terephthalate nanoparticles by a polyester hydrolase from *Thermobifida fusca*. Biochem Eng J 2015;93:222–8. https://doi.org/10.1016/J.BEJ.2014.10.012.
[82] Arnling Bååth J, Borch K, Jensen K, Brask J, Westh P. Comparative biochemistry of four polyester (PET) hydrolases. ChemBioChem 2021;22:1627–37. https://doi.org/10.1002/cbic.202000793.
[83] Wei R, Breite D, Song C, Gräsing D, Ploss T, Hille P, et al. Biocatalytic degradation efficiency of postconsumer polyethylene terephthalate packaging determined by their polymer microstructures. Adv Sci 2019;6:1900491. https://doi.org/10.1002/advs.201900491.
[84] Chang AC, Patel A, Perry S, Soong YV, Ayafor C, Wong HW, et al. Understanding consequences and tradeoffs of melt processing as a pretreatment for enzymatic depolymerization of poly(ethylene terephthalate). Macromol Rapid Commun 2022;43:e2100929. https://doi.org/10.1002/marc.202100929.
[85] Thomsen TB, Schubert S, Hunt CJ, Borch K, Jensen K, Brask J, et al. Rate response of poly(ethylene terephthalate)-hydrolases to substrate crystallinity: Basis for understanding the lag phase. ChemSusChem 2023;16:e202300291. https://doi.org/10.1002/cssc.202300291.
[86] Tarazona NA, Wei R, Brott S, Pfaff L, Bornscheuer UT, Lendlein A, et al. Rapid depolymerization of poly(ethylene terephthalate) thin films by a dual-enzyme system and its impact on material properties. Chem Catal 2022;2:3573–89. https://doi.org/10.1016/j.checat.2022.11.004.
[87] Sonnendecker C, Oeser J, Richter PK, Hille P, Zhao Z, Fischer C, et al. Low carbon footprint recycling of post-consumer PET plastic with a metagenomic polyester hydrolase. ChemSusChem 2022;15:e202101062. https://doi.org/10.1002/cssc.202101062.
[88] Frank R, Krinke D, Sonnendecker C, Zimmermann W, Jahnke HG. Real-time noninvasive analysis of biocatalytic PET degradation. ACS Catal 2022;12:25–35. https://doi.org/10.1021/acscatal.1c03963.
[89] Lippold H, Kahle L, Sonnendecker C, Matysik J, Fischer C. Temporal and spatial evolution of enzymatic degradation of amorphous PET plastics. Npj Mater Degrad 2022;6:1–6. https://doi.org/10.1038/s41529-022-00305-6.
[90] Arnal G, Anglade J, Gavalda S, Tournier V, Chabot N, Bornscheuer UT, et al. Assessment of four engineered PET degrading enzymes considering large-scale industrial applications. ACS Catal 2023;13:13156–66. https://doi.org/10.1021/acscatal.3c02922.
[91] Weinberger S, Haernvall K, Scaini D, Ghazaryan G, Zumstein MT, Sander M, et al. Enzymatic surface hydrolysis of poly(ethylene furanoate) thin films of various crystallinities. Green Chem 2017;19:5381–4. https://doi.org/10.1039/c7gc02905e.
[92] Wallace NE, Adams MC, Chafin AC, Jones DD, Tsui CL, Gruber TD. The highly crystalline PET found in plastic water bottles does not support the growth of the PETase-producing bacterium *Ideonella sakaiensis*. Environ Microbiol Rep 2020;12:578–82. https://doi.org/10.1111/1758-2229.12878.
[93] Erickson E, Shakespeare TJ, Bratti F, Buss BL, Graham R, Hawkins MA, et al. Comparative performance of PETase as a function of reaction conditions, substrate properties, and product accumulation. ChemSusChem 2022;15:e202101932. https://doi.org/10.1002/CSSC.202101932.
[94] Arnling Bååth J, Borch K, Westh P. A suspension-based assay and comparative detection methods for characterization of polyethylene terephthalate hydrolases. Anal Biochem 2020:607. https://doi.org/10.1016/j.ab.2020.113873.
[95] Brizendine RK, Erickson E, Haugen SJ, Ramirez KJ, Miscall J, Pickford AR, et al. Particle size reduction of poly(ethylene terephthalate) increases the rate of enzymatic depolymerization but does not increase the overall conversion extent. ACS Sustain Chem Eng 2022;10:9131–49. https://doi.org/10.1021/acssuschemeng.2c01961.
[96] Kaabel S, Daniel Therien JP, Deschênes CE, Duncan D, Friščic T, Auclair K. Enzymatic depolymerization of highly crystalline polyethylene terephthalate enabled in moist-solid reaction mixtures. Proc Natl Acad Sci USA 2021;118:e2026452118. https://doi.org/10.1073/pnas.2026452118.
[97] Guo B, Vanga SR, Lopez-Lorenzo X, Saenz-Mendez P, Ericsson SR, Fang Y, et al. Conformational selection in biocatalytic plastic degradation by PETase. ACS Catal 2022;12:3397–409. https://doi.org/10.1021/acscatal.1c05548.
[98] Erickson E, Gado JE, Avilán L, Bratti F, Brizendine RK, Cox PA, et al. Sourcing thermotolerant poly(ethylene terephthalate) hydrolase scaffolds from natural diversity. Nat Commun 2022:13. https://doi.org/10.1038/s41467-022-35237-x.
[99] Zhang Y, Zhang J, Lu Y, Duan Y, Yan S, Shen D. Glass transition temperature determination of poly(ethylene terephthalate) thin films using reflection−absorption FTIR. Macromolecules 2004;37:2532–7. https://doi.org/10.1021/MA035709F.
[100] Shinotsuka K, Bliznyuk VN, Assender HE. Near-surface crystallization of PET. Polym (Guildf) 2012;53:5554–9. https://doi.org/10.1016/J.POLYMER.2012.09.048.
[101] Zuo B, Liu Y, Liang Y, Kawaguchi D, Tanaka K, Wang X. Glass transition behavior in thin polymer films covered with a surface crystalline layer. Macromolecules 2017;50:2061–8. https://doi.org/10.1021/acs.macromol.6b02740.
[102] Ding Z, Xu G, Miao R, Wu N, Zhang W, Yao B, et al. Rational redesign of thermophilic PET hydrolase LCC_{ICCG} to enhance hydrolysis of high crystallinity polyethylene terephthalates. J Hazard Mater 2023;453:131386. https://doi.org/10.1016/j.jhazmat.2023.131386.
[103] Ronkvist ÅM, Lu W, Feder D, Gross RA. Cutinase-catalyzed deacetylation of poly (vinyl acetate. Macromolecules 2009;42:6086–97. https://doi.org/10.1021/ma900530j.
[104] Pfaff L, Gao J, Li Z, Jäckering A, Weber G, Mican J, et al. Multiple substrate binding mode-guided engineering of a thermophilic PET hydrolase. ACS Catal 2022;12:9790–800. https://doi.org/10.1021/acscatal.2c02275.
[105] Sagong HY, Son HF, Seo H, Hong H, Lee D, Kim KJ. Implications for the PET decomposition mechanism through similarity and dissimilarity between PETases from *Rhizobacter gummiphilus* and *Ideonella sakaiensis*. J Hazard Mater 2021;416:126075. https://doi.org/10.1016/j.jhazmat.2021.126075.
[106] Makryniotis K, Nikolaivits E, Gkountela C, Vouyiouka S, Topakas E. Discovery of a polyesterase from *Deinococcus maricopensis* and comparison to the benchmark LCC_{ICCG} suggests high potential for semi-crystalline post-consumer PET degradation. J Hazard Mater 2023;455:131574. https://doi.org/10.1016/j.jhazmat.2023.131574.
[107] Yong AXH, Sims GD, Gnaniah SJP, Ogin SL, Smith PA. Heating rate effects on thermal analysis measurement of Tg in composite materials. Adv Manuf Polym Compos Sci 2017;3:43–51. https://doi.org/10.1080/20550340.2017.1315908.
[108] Wellen RMR, Rabello MS. The kinetics of isothermal cold crystallization and tensile properties of poly(ethylene terephthalate. J Mater Sci 2005;40:6099–104. https://doi.org/10.1007/s10853-005-3173-3.
[109] Ellis LD, Rorrer NA, Sullivan KP, Otto M, McGeehan JE, Román-Leshkov Y, et al. Chemical and biological catalysis for plastics recycling and upcycling. Nat Catal 2021;4:539–56. https://doi.org/10.1038/s41929-021-00648-4.
[110] Tournier V, Duquesne S, Guillamot F, Cramail H, Taton D, Marty A, et al. Enzymes' power for plastics degradation. Chem Rev 2023;123:5612–70. https://doi.org/10.1021/acs.chemrev.2c00644.
[111] WTS Global. Plastic Taxation in Europe: Update 2023. Available at: https://Wts.Com/Global/Publishing-Article/20230522-Plastic-Taxation-Europe-Update-2023~publishing-Article: 2023.
[112] Sammon C, Yarwood J, Everall N. A FTIR-ATR study of liquid diffusion processes in PET films: comparison of water with simple alcohols. Polymer 2000;41:2521–34. https://doi.org/10.1016/S0032-3861(99)00405-X.